AN IMPROVED QUADRATURE RULE FOR THE FLUX-COMPUTATION IN STAGGERED CENTRAL DIFFERENCE SCHEMES IN MULTIDIMENSIONS

KNUT–ANDREAS LIE AND SEBASTIAN NOELLE

ABSTRACT. We present a new second-order, nonoscillatory, central difference scheme on two-dimensional, staggered, Cartesian grids for systems of conservation laws. The scheme uses a new, carefully designed integration rule for the flux computations and thereby takes more propagation directions into account. This effectively reduces grid orientation effects produced for two-dimensional radially symmetric gas flows and improves the accuracy for smooth solutions.

1. INTRODUCTION

The nonoscillatory, central difference scheme introduced by Nessyahu and Tadmor [2] (NT scheme) is a second order extension of the classical Lax-Friedrichs (LxF) scheme [1]. Both the LxF and the NT schemes can be seen as Godunov-type central schemes using staggered grids. The NT scheme has proved to be an efficient computational method for systems of conservation laws in one spatial dimension. Since the scheme applies no characteristic information or Riemann solvers, it yields especially compact and simple computer code and can easily be applied to systems for which no Riemann solver exists.

Here we consider systems of hyperbolic conservation laws in two spatial dimensions

$$u_t + f(u)_x + g(u)_y = 0, \qquad u(x,0) = u_0(x), \tag{1}$$

where $u : \mathbb{R}^2 \times \mathbb{R}_+ \to \mathbb{R}^m$ is the vector of conservative variables and $f, g : \mathbb{R}^m \to \mathbb{R}^m$ are the fluxes in x- and y-direction. Prototypes of these equations are the Euler equations of gas dynamics, the shallow water equations, and the equations of ideal magnetohydrodynamics, to name a few.

The Nessyahu–Tadmor scheme was extended to Cartesian grids in two spatial dimensions by Arminjon et al. [3] and by Jiang and Tadmor [4]. Here we will review this two-dimensional extension of the NT scheme (abbreviated hereafter NT2d) with special emphasis on the quadrature rules for the fluxes across the boundaries of the staggered cells. The fluxes are evaluated in the corners of these cells, which lie in the interior of cells of the original grid. The fluxes computed to the x- and y-directions add up to a single flux to the diagonal direction, and only the four diagonal directions are effectively used in the NT2d scheme. We present a radially symmetric explosion problem in gas dynamics for which the scheme clearly produces grid orientation effects. This motivates the derivation of a new staggered scheme that takes twice as many propagation directions into account. This is achieved by introducing a carefully designed integration rule for the flux computations. The new scheme, which is easily extended to three and more spatial dimensions, has less grid orientation effects and preserves symmetries better than the original scheme at the expense of a somewhat higher runtime. This is demonstrated for the radially symmetric test problem, for which (almost)

The research was funded in part by the BeMatA program of the Research Council of Norway.

all directional effects are eliminated. Moreover, the new scheme gives decreased errors and improved convergence rates for a test case of oblique, linear advection.

2. Flux Computations in the two-dimensional Nessyahu–Tadmor Scheme

Define the points in a regular Cartesian grid by $x_j = j\Delta x$, $y_k = k\Delta y$ and $t_n = n\Delta t$, $j,k \in \mathbb{Z}$, $n \in \mathbb{N}$. The NT2d scheme approximates cell-averages of the solution on two sets of grids, the *original* and the *staggered*, respectively:

$$C_{j,k} = [x_{j-\frac{1}{2}}, x_{j+\frac{1}{2}}] \times [y_{k-\frac{1}{2}}, y_{k+\frac{1}{2}}], \qquad C_{j+\frac{1}{2},k+\frac{1}{2}} = [x_j, x_{j+1}] \times [y_k, y_{k+1}].$$

At even time-steps the solution is given as a piecewise linear function over the *original* grid,

$$\overline{w}(x,y,t_n) = \overline{w}^{\,n}_{jk} + \frac{x-x_j}{\Delta x} w'_{jk} + \frac{y-y_k}{\Delta y} w^{\backprime}_{jk} \quad \text{for} \quad (x,y) \in C_{jk}. \tag{2}$$

The values $\overline{w}^{\,n}_{jk}$ are cell-averages and the finite-difference operators $' \approx \Delta x \frac{\partial}{\partial_x}$ and $^{\backprime} \approx \Delta y \frac{\partial}{\partial_y}$ are realised by piecewise linear reconstructions with standard limiter-functions, which are applied to each component of the vectors (see (8), (9) and (15) below).

For the next time step, the NT2d scheme updates $\overline{w}^{\,n+1}_{j+1/2,k+1/2}$ at time t_{n+1} over the *staggered* cells as

$$\begin{aligned}
\overline{w}^{\,n+1}_{j+\frac{1}{2},k+\frac{1}{2}} =& \frac{1}{4}\left(\overline{w}^{\,n}_{jk} + \overline{w}^{\,n}_{j+1,k} + \overline{w}^{\,n}_{j+1,k+1} + \overline{w}^{\,n}_{j,k+1}\right) \\
&+ \frac{1}{16}\left(w'_{jk} + w'_{j,k+1} - w'_{j+1,k} - w'_{j+1,k+1}\right) \\
&+ \frac{1}{16}\left(w^{\backprime}_{jk} - w^{\backprime}_{j,k+1} + w^{\backprime}_{j+1,k} - w^{\backprime}_{j+1,k+1}\right) \\
&- \frac{\lambda}{2}\Big[f(w^{n+\frac{1}{2}}_{j+1,k}) + f(w^{n+\frac{1}{2}}_{j+1,k+1})\Big] + \frac{\lambda}{2}\Big[f(w^{n+\frac{1}{2}}_{j,k}) + f(w^{n+\frac{1}{2}}_{j,k+1})\Big] \\
&- \frac{\mu}{2}\Big[g(w^{n+\frac{1}{2}}_{j+1,k+1}) + g(w^{n+\frac{1}{2}}_{j,k+1})\Big] + \frac{\mu}{2}\Big[g(w^{n+\frac{1}{2}}_{j+1,k}) + g(w^{n+\frac{1}{2}}_{j,k})\Big],
\end{aligned} \tag{3}$$

where $\lambda = \Delta t/\Delta x$, $\mu = \Delta t/\Delta y$, and

$$w^{n+\frac{1}{2}}_{jk} = \overline{w}^{\,n}_{jk} - \frac{\lambda}{2} f'_{jk} - \frac{\mu}{2} g^{\backprime}_{jk} \tag{4}$$

is a predictor step in the centres of the non-staggered cells at time $t_{n+1/2}$. This predictor step uses the conservation law (1) to approximate the time derivative of w.

Let us take a closer look at formula (3). The first three lines on the right-hand-side give the cell-average of the reconstruction $\overline{w}(\cdot, t_n)$ in (2) over the staggered cell $C_{j+\frac{1}{2},k+\frac{1}{2}}$. The following two lines approximate the integral of the fluxes across the boundaries of the cell from time t_n to t_{n+1} by a quadrature rule in space-time. For example, over the left of the staggered control volume the space-time quadrature used in (3) is

$$\frac{1}{\Delta y \Delta t} \int_{y_k}^{y_{k+1}} \int_{t_n}^{t_{n+1}} f(w(x_j,y,t))\, dy\, dt \approx \frac{1}{2}\Big(f\big(w^{n+\frac{1}{2}}_{jk}\big) + f\big(w^{n+\frac{1}{2}}_{j,k+1}\big)\Big). \tag{5}$$

This quadrature consists of the midpoint rule in time and the trapezoidal rule in space. The nodes of the quadrature rule are (see Figure 2(a) on page 6)

$$(x_j, y_k, t_{n+1/2}),\ (x_j, y_{k+1}, t_{n+1/2}). \tag{6}$$

These points lie on the interface of the *staggered* grid and above the *centres* of the original grid cells. Here the reconstruction (2) is *smooth*. Moreover, the solution of (1) with initial data (2) given at time t_n will remain smooth along $(x_j, y_k) \times [t_n, t_{n+1}]$ as long as the CFL condition

$$\Delta t \ \max\Big(\frac{a_{\max}}{\Delta x}, \frac{b_{\max}}{\Delta y}\Big) < \frac{1}{2} \tag{7}$$

is satisfied. (Here $a_{\max}$ and $b_{\max}$ denote maximal speeds of propagation in the x- and y-directions). It is therefore justified to approximate the solution at $(x_j, y_k, t_{n+1/2})$ using Taylor expansions and the conservation law (1) as in (4). As a consequence, no one-dimensional characteristic decompositions of the flux-vectors are needed, which makes the scheme particularly simple to implement.

In [4, Table 4.4] a numerical experiment for a non-standard weakly hyperbolic system shows particularly convincing numerical results for a boundary value problem with an underlying radially symmetric solution. The following example demonstrates that the NT2d scheme may exhibit visible grid-orientation effects in other cases: Consider the Euler equations for an ideal gas with gas constant $\gamma = 1.4$. Let the initial data be

$$(\rho, u, v, p)(x, y, 0) = \begin{cases} (1.0, 0, 0, 1.0), & |x|^2 + |y|^2 \le 0.16 \\ (0.0125, 0, 0, 0.1), & \text{otherwise.} \end{cases}$$

The solution consists of a circular shock wave propagating outwards from the origin, followed by a contact discontinuity, and a rarefaction wave travelling towards the origin.

To limit numerical derivatives (as in (2)) we use the smooth CWENO (Central Weighted Essentially Non-Oscillatory, see [5] for the derivation and further references) limiter

$$w'_{jk} = \mathrm{CWENO}\big(\overline{w}^{\,n}_{jk} - \overline{w}^{\,n}_{j-1,k}\,, \overline{w}^{\,n}_{j+1,k} - \overline{w}^{\,n}_{jk}\big) \tag{8}$$

$$\mathrm{CWENO}(a, b) = \frac{w(a)\cdot a + w(b)\cdot b}{w(a) + w(b)}, \qquad w(a) = \big(\varepsilon + a^2\big)^{-2},\ \varepsilon = 10^{-6}. \tag{9}$$

Note that in [5], the authors base their CWENO reconstruction on three piecewise quadratic polynomials and eventually design a fourth order accurate scheme. Here we are only interested in second order schemes, so we work with two piecewise linear ansatz functions.

Figure 1 shows a scatter plot of the solution at time $t = 0.2$ computed by the original NT2d scheme. In the current setting, a scatter plot for a given physical quantity is a plot of the value in each grid cell versus the distance of the cell centre from the origin. In this way we can present the spread in the data, as a solution with perfect radial symmetry would consist of points lying on a single line.

Although the scheme gives relatively sharp resolution of the shock and the rarefaction wave (the shock is 2–3 computational cells wide for each one-dimensional cross-section of the numerical solution), it suffers from grid orientation effects. This is particularly evident for the internal energy in the zone between the shock and the contact discontinuity. Moreover, slight overshoots in pressure and radial velocity can be observed behind the leading shock in regions close to the diagonal lines $x = \pm y$. Similar grid orientation effects were observed for other limiters as well, e.g., van Leer, minmod limiters (MM_1 and MM_2) and superbee. The more compressive the limiter, the stronger the grid orientation effects.

3. An Improved Quadrature Rule

The presence of grid orientation effects observed in computations on radially symmetric solutions (as demonstrated above, for instance) motivated us to look for a modification of the NT2d scheme that would reduce these directional effects.

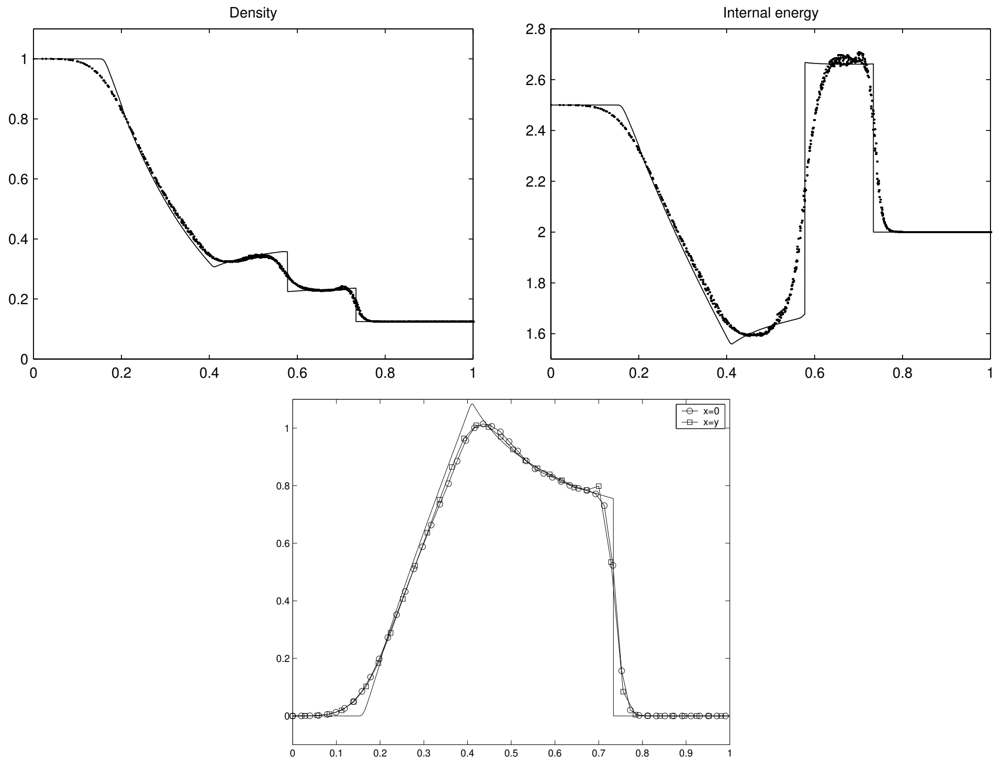

FIGURE 1. Solution at time $t = 0.2$ of the cylindrical explosion problem computed by the original NT2d scheme on a 101×101 grid with CWENO limiter and CFL number 0.475; (top) scatter plots, (bottom) plots of radial velocity component along two cross sections.

Here is our new scheme: We propose to replace (3) by

$$
\begin{aligned}
\overline{w}^{\,n+1}_{j+\frac12,k+\frac12} =& \frac14\big(\overline{w}^{\,n}_{jk} + \overline{w}^{\,n}_{j+1,k} + \overline{w}^{\,n}_{j+1,k+1} + \overline{w}^{\,n}_{j,k+1}\big) \\
&+ \frac{1}{16}\big(w'_{jk} + w'_{j,k+1} - w'_{j+1,k} - w'_{j+1,k+1}\big) \\
&+ \frac{1}{16}\big(w^{\backprime}_{jk} - w^{\backprime}_{j,k+1} + w^{\backprime}_{j+1,k} - w^{\backprime}_{j+1,k+1}\big) \\
&- \frac{\lambda}{4}\Big[f(w^{n+1}_{j+1,k}) + f^{n,-}_{j+1,k+\frac12} + f^{n,+}_{j+1,k+\frac12} + f(w^{n+1}_{j+1,k+1})\Big] \\
&+ \frac{\lambda}{4}\Big[f(w^{n+1}_{jk}) + f^{n,-}_{j,k+\frac12} + f^{n,+}_{j,k+\frac12} + f(w^{n+1}_{j,k+1})\Big] \\
&- \frac{\mu}{4}\Big[g(w^{n+1}_{j,k+1}) + g^{n,-}_{j+\frac12,k+1} + g^{n,+}_{j+\frac12,k+1} + g(w^{n+1}_{j+1,k+1})\Big] \\
&+ \frac{\mu}{4}\Big[g(w^{n+1}_{jk}) + g^{n,-}_{j+\frac12,k} + g^{n,+}_{j+\frac12,k} + g(w^{n+1}_{j+1,k})\Big],
\end{aligned}
\tag{10}
$$

where

$$
w^{n+1}_{jk} = \overline{w}^{\,n}_{jk} - \lambda f'_{jk} - \mu g^{\backprime}_{jk}
\tag{11}
$$

and

$$
\begin{aligned}
f^{n,-}_{j,k+\frac{1}{2}} &= f(\overline{w}^{\,n}_{jk} + \frac{1}{2} w^{\backprime}_{jk}), \qquad & f^{n,+}_{j,k+\frac{1}{2}} &= f(\overline{w}^{\,n}_{j,k+1} - \frac{1}{2} w^{\backprime}_{j,k+1}), \\
g^{n,-}_{j+\frac{1}{2},k} &= g(\overline{w}^{\,n}_{jk} + \frac{1}{2} w'_{jk}), \qquad & g^{n,+}_{j+\frac{1}{2},k} &= g(\overline{w}^{\,n}_{j+1,k} - \frac{1}{2} w'_{j+1,k}).
\end{aligned}
\tag{12}
$$

The difference between our new scheme (10)–(12), which we abbreviate LN2d hereafter, and the NT2d scheme (3)–(4) is a new quadrature rule in the computation of the fluxes across the sides. For example, the quadrature rule for the left side of the staggered control volume corresponding to (5) is now

$$
\frac{1}{\Delta y \Delta t} \int_{y_k}^{y_{k+1}} \int_{t_n}^{t_{n+1}} f(w(x_j, y, t))\, dy\, dt \approx
\frac{1}{4} \Big(f\big(w^{n,-}_{j,k+\frac{1}{2}}\big) + f\big(w^{n,+}_{j,k+\frac{1}{2}}\big) + f\big(w^{n+1}_{jk}\big) + f\big(w^{n+1}_{j,k+1}\big) \Big).
\tag{13}
$$

The nodes of this quadrature rule are (see Figure 2(b)).

$$
(x_j, y_{k+\frac{1}{2}}, t_n), \quad (x_j, y_k, t_{n+1}), \quad (x_j, y_{k+1}, t_{n+1}).
$$

At the first quadrature point the reconstruction $\overline{w}(\cdot, t_n)$ is now *discontinuous*, so we have to evaluate the fluxes at the *one-sided* limits as in (12).

As long as the CFL condition (7) is satisfied, the quadrature points at time t_{n+1} still lie within the domain of smoothness of the solution to (1) with initial data (2). Therefore it is justified to extrapolate the solution using Taylor series as in (11).

The main advantage of the new quadrature is that it takes *twice as many directions* into account: while the original NT2d scheme effectively uses only the four diagonal directions in the flux computation, LN2d uses the diagonal directions *and* the grid-directions themselves. To see this, let us have a look at the "floorplan" of the two schemes in Figure 3. The NT2d scheme evaluates all fluxes at the corners of the staggered cell. If we multiply (3) by $\Delta x \Delta y / \Delta t$ and collect the fluxes at the quadrature point $(x_{j+1}, y_{k+1}, t_{n+1/2})$ in the north-east corner, we obtain a contribution of

$$
\frac{\Delta y}{2} f(w^{n+\frac{1}{2}}_{j+1,k+1}) + \frac{\Delta x}{2} g(w^{n+\frac{1}{2}}_{j+1,k+1})
$$

to the flux across the boundary of the cell. This adds up to evaluating the normal flux in the direction

$$
n_{\mathrm{NE}} = (\Delta y, \Delta x)/(\Delta x^2 + \Delta y^2)^{\frac{1}{2}}.
$$

Similar contributions arise at the north-west, south-west and south-east corners. For a square grid, these are the diagonal directions, and for a general Cartesian grid, the directions normal to the diagonal directions, see Figure 3(a). This leads us to a reinterpretation of the NT2d scheme: rather than evaluating fluxes across the *sides* of the staggered cells, it computes fluxes across its *corners*. The grid directions themselves are not taken into account.

The LN2d scheme (10) uses two sets of quadrature points, those at the old time t_n in the centres of the sides, where fluxes are computed to the grid directions, and those at time t_{n+1} in the corners, where fluxes are computed into the diagonal directions as for the NT2d scheme. Therefore, we now have eight directions in two space-dimensions instead of four for the NT2d scheme, see Figure 3(b).

For the exact solution of a multi-dimensional hyperbolic system, there are infinitely many directions of wave-propagation. Our heuristical argument is that the numerical approximation of multi-dimensional waves should be improved if one increases the number of propagation

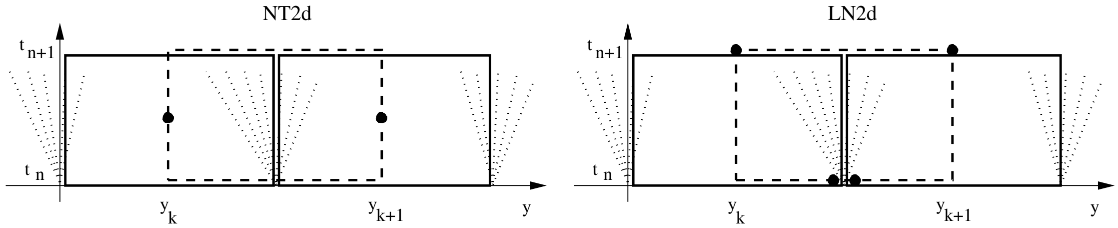

FIGURE 2. Quadrature points for the fluxes over the left side of the staggered control volume, shown in the (y, t)-plane. The dashed rectangles are cells of the staggered grid, while the solid rectangles are the sides of the original grid. The dotted lines symbolise Riemann-fans originating from the cell-boundaries of the original grid.

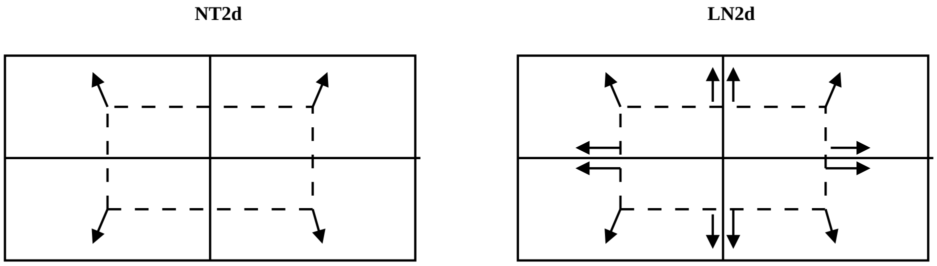

FIGURE 3. Floor-plan of the staggered schemes in the (x, y)-plane. The solid lines symbolise the original cells C_{jk}, the dashed line the staggered cell $C_{j+\frac{1}{2},k+\frac{1}{2}}$, and the arrows the fluxes across its boundaries.

directions which are involved in the computation of the numerical fluxes. For the NT2d and LN2d schemes considered here, we can back up this heuristics with numerical evidence. As we shall show below, our new LN2d scheme does reduce grid orientation effects for the radially symmetric flow computed above with the NT2d scheme.

To obtain more propagation directions, we must pay the price of more flux evaluations, thus making the scheme computationally more expensive. At a first glance, 16 flux evaluations are needed in (10), as compared with only 8 in (3). However, fluxes at the corners can be recycled four times for the adjacent cells, and fluxes at the sides can be used twice. This gives an effective count of 6 flux evaluations for the LN2d scheme and 2 for the NT2d scheme. Fortunately, the additional flux-evaluations in (10) can be completely avoided by setting

$$f^{n,-}_{j,k+\frac{1}{2}} = f(\overline{w}^{\,n}_{jk}) + \frac{1}{2} f'_{jk} \qquad f^{n,+}_{j,k+\frac{1}{2}} = f(\overline{w}^{\,n}_{j,k+1}) - \frac{1}{2} f'_{j,k+1} \tag{14}$$

and similarly for $g^{n,-}$ and $g^{n,+}$. Equation (14) is exact for linear flux functions. Therefore all additional work needed is to compute f' and g' at time t_n at the centres of the original cells C_{jk}.

Let us briefly sketch how to extend these ideas to higher spatial dimensions. For a d-dimensional Cartesian grid, one can easily define a second order staggered scheme analogous to (3). The quadrature rule analogous to (5) over one of the $(d-1)$-dimensional faces of a d-dimensional cell will be the average of the fluxes normal to the face, evaluated at the 2^{d-1} corners at time $t^{n+1/2}$. At each corner, d faces meet, and the sum of the respective fluxes will always point into a diagonal direction of the grid. In this sense, the fluxes in the grid directions are not used in the scheme. The analogue of our new quadrature rule adds one spatial quadrature point for each face, namely the center of the face. Due to the staggering of the grid, the solution at this point consists of 2^{d-1} discontinuous pieces. We average the corresponding normal fluxes at time t^n, and average this with the average of the normal fluxes at the corners at time t^{n+1}. This yields the analogue of formula (13). As in the two-dimensional case, the new scheme will take the diagonal directions *and* the grid directions into account.

Similarly as in [4, Theorem 1], we can prove the following local maximum principle for the new two-dimensional scheme (10), (11), (14):

Theorem 1. *Consider the scheme* (10), (11) *and* (14) *where all discrete derivatives are limited by the minmod-limiter* [4, (3.1)], *i.e.,*

$$w'_{jk} = \mathrm{MM}\big(\theta(\overline{w}^{\,n}_{j+1,k} - \overline{w}^{\,n}_{jk}), \tfrac{1}{2}(\overline{w}^{\,n}_{j+1,k} - \overline{w}^{\,n}_{j-1,k}), \theta(\overline{w}^{\,n}_{jk} - \overline{w}^{\,n}_{j-1,k})\big), \qquad 1 \le \theta \le 2. \tag{15}$$

Suppose that the CFL-condition

$$\Delta t \; \max\Big(\frac{a_{\max}}{\Delta x}, \frac{b_{\max}}{\Delta y}\Big) \le C_\theta \tag{16}$$

holds, where the CFL-number C_θ is given by

$$C_\theta = -\frac{2+\theta}{6\,\theta} + \sqrt{\Big(\frac{2+\theta}{6\,\theta}\Big)^2 + \frac{2-\theta}{12\,\theta}}. \tag{17}$$

Then the update $\overline{w}^{\,n+1}_{j+\frac{1}{2},k+\frac{1}{2}}$ satisfies the local maximum principle

$$\min_{j',k'=0,1} \overline{w}^{\,n}_{j+j',k+k'} \le \overline{w}^{\,n+1}_{j+\frac{1}{2},k+\frac{1}{2}} \le \max_{j',k'=0,1} \overline{w}^{\,n}_{j+j',k+k'}. \tag{18}$$

Note that the CFL-condition (17) is slightly more restrictive than the one in [4]. For example, for $\theta = 1$ we obtain $C_1 = 1/\sqrt{3} - 1/2 \approx 0.077$, as opposed to $C_1 = (\sqrt{7}-2)/6 \approx 0.1076$ for the NT2d scheme. For $\theta = 2$, $C_2 = 0$, as in [4].

Let us now revisit the radially symmetric Sod problem discussed above and recompute the approximate solution using LN2d with exactly the same parameters as in Figure 1. Figure 4 shows a scatter plot of the corresponding solution at time $t = 0.2$. Now, most of the directional effects have disappeared, in particular the overshoots in pressure and radial velocity immediately behind the leading shock. Use of the new quadrature rule also removes grid orientation effects observed for other limiters (e.g., minmod, van Leer, superbee). The improvement in radial symmetry is more pronounced the more compressive the limiter is and the higher the CFL number is.

Table 1 gives L^1-errors and runtimes for the two schemes on a series of refined grids. The errors are computed relative to the cell average projection of an accurate front tracking solution of the corresponding reduced one-dimensional, inhomogeneous problem. Although LN2d gives improved accuracy for each given number of grid points, the NT2d scheme is more efficient in terms of achieved accuracy per unit CPU time except on the finest grid, see Figure 5.

Finally, we include a study of the accuracy of LN2d for two different problems with smooth solutions and make comparisons with NT2d. For each problem we use periodic boundary conditions and compute the error on a series of refined grids using fixed CFL number 0.3. The first example is an oblique, linear advection $u_t + u_x + u_y = 0$ with initial data $\sin(\pi(x+y))$ as in [4]. Runtimes and L^1-errors measured at time $t = 2.0$ are given in Table 2. The second example is the Euler equations on the unit square subject to initial conditions

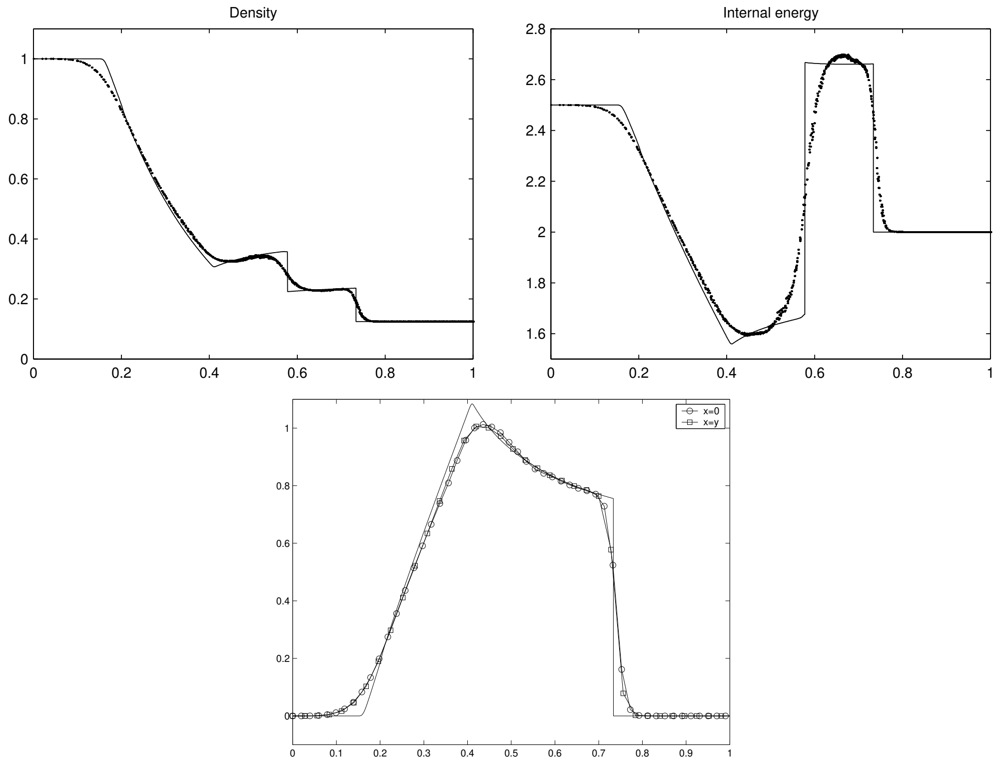

FIGURE 4. Solution at time $t = 0.2$ of the cylindrical explosion problem computed by LN2d on a 101×101 grid with CWENO limiter and CFL number 0.475; (top) scatter plots, (bottom) plots of radial velocity component along two cross sections.

TABLE 1. *Runtime and L^1-errors for NT2d (top half) and LN2d (bottom half) with CFL number 0.4 on a series of refined $N \times N$ grids.*

N	ρ	ρu_r	E	p	u_r	CPU
32	6.588e-02	5.043e-02	1.354e-01	1.701e-01	5.682e-02	0.2
64	4.056e-02	3.047e-02	7.697e-02	8.568e-02	3.071e-02	1.8
128	2.194e-02	1.739e-02	4.055e-02	4.524e-02	1.628e-02	14.9
256	1.223e-02	1.000e-02	2.155e-02	2.252e-02	8.294e-03	123.4
512	5.756e-03	4.327e-03	1.017e-02	1.032e-02	3.929e-03	782.6
32	6.377e-02	4.790e-02	1.314e-01	1.608e-01	5.594e-02	0.3
64	4.046e-02	2.935e-02	7.393e-02	8.182e-02	2.966e-02	2.8
128	2.144e-02	1.664e-02	3.905e-02	4.455e-02	1.581e-02	22.4
256	1.194e-02	9.636e-03	2.081e-02	2.226e-02	8.044e-03	192.8
512	4.719e-03	3.303e-03	8.640e-03	9.162e-03	3.490e-03	1282.8

$(\rho, u, v, p) = \big(1 + 0.1\cos(2\pi x)\cos(2\pi y), cos(\theta), \sin(\theta), 1\big)$ for $\theta = 0.1\pi$. Runtimes and L^1-error of ρ component measured at time $t = 0.5$ are given in Table 3.

The improved flux quadrature decreases the errors and improves the convergence rates at the cost of an about 50% increase in the runtime. A comparison of the efficiency of the schemes shows that LN2d is more efficient than NT2d on the finer grids in both examples, see Figure 6. Moreover, it seems that for the scalar examples, the LN2d scheme is even

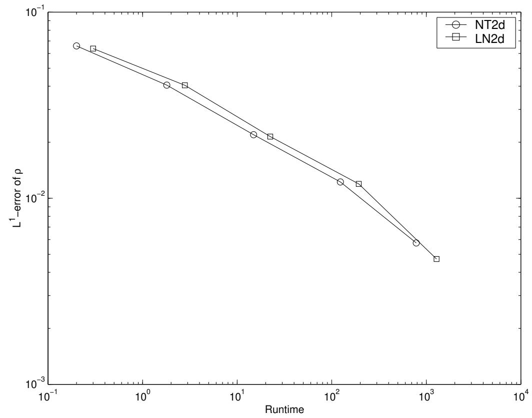

FIGURE 5. Comparison of efficiency for NT2d and LN2d for the grid refinement study in Table 1.

TABLE 2. *Grid refinement study for the oblique, linear advection example on a series of $N \times N$ grids; τ denotes the ratio of the runtimes of LN2d and NT2d.*

	NT2d			LN2d			
N	L^1-error	rate	CPU	L^1-error	rate	CPU	τ
40	9.76e-02	—	0.5	1.14e-01	—	0.7	1.40
80	2.66e-02	1.9	4.1	2.90e-02	2.0	6.2	1.51
160	6.78e-03	2.0	39.0	6.13e-03	2.2	59.3	1.52
320	1.55e-03	2.1	321.9	8.03e-04	2.9	485.0	1.51
640	3.46e-04	2.2	2571.0	8.20e-05	3.3	3951.0	1.54

TABLE 3. *Grid refinement study for the oblique Euler flow on a series of $N \times N$ grids; τ denotes the ratio of the runtimes of LN2d and NT2d.*

	NT2d			LN2d			
N	L^1-error	rate	CPU	L^1-error	rate	CPU	τ
40	2.74e-03	—	2.0	2.64e-03	—	2.9	1.45
80	4.43e-04	2.6	18.9	4.01e-04	2.7	28.1	1.49
160	5.09e-05	3.1	150.9	3.31e-05	3.6	226.7	1.50
320	9.61e-06	2.4	1208.2	3.76e-06	3.1	1911.8	1.58
640	2.35e-06	2.0	9907.4	8.29e-07	2.2	15891.8	1.60

superconvergent (with rates higher than two on the finer grids). Obviously, we do not expect this to happen for general test problems.

REFERENCES

[1] P. Lax. Weak solutions of nonlinear hyperbolic equations and their numerical computation. *Comm. Pure Appl. Math.* 7:159–193, 1954.
[2] H. Nessyahu and E. Tadmor. Non-oscillatory central differencing for hyperbolic conservation laws. *J. Comput. Phys.* 87:408–463, 1990.
[3] P. Arminjon, D. Stanescu and M.-C. Viallon. A two-dimensional finite volume extension of the Lax–Friedrichs and Nessyahu-Tadmor schemes for compressible flows. *Proc. 6th. Int. Symp. on CFD, Lake Tahoe* M. Hafez and K. Oshima (eds.) , Vol. IV, pp. 7–14, 1995.

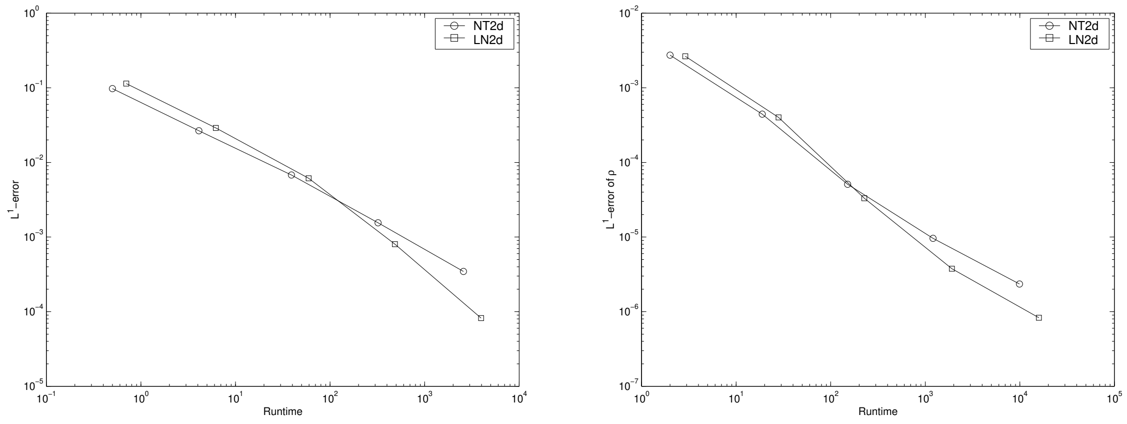

FIGURE 6. Comparison of efficiency for NT2d and LN2d for the grid refinement studies in Tables 2 (left) and 3 (right).

[4] G.-S. Jiang and E. Tadmor. Nonoscillatory central schemes for multidimensional hyperbolic conservation laws. *SIAM J. Sci. Comput.* 19(6):1892–1917 (electronic), 1998.

[5] D. Levy, G. Puppo and G. Russo. Central WENO Schemes for Hyperbolic Systems of Conservation Laws. *Math. Mod. Num. Anal. (MMAN)* 33(3):547–571, 1999.

(Knut–Andreas Lie) SINTEF Applied Mathematics, P.0. Box 124 Blindern, N–0314 Oslo, Norway. Also: Scientific Computing Group, Department of Informatics, University of Oslo

E-mail address: Knut-Andreas.Lie@math.sintef.no

URL: http://www.ifi.uio.no/~kalie/

(Sebastian Noelle) Institut für Geometrie und Praktische Mathematik, RWTH Aachen, D-52056 Aachen, Germany

E-mail address: noelle@igpm.rwth-aachen.de

URL: http://www.igpm.rwth-aachen.de/~noelle/